Signature of HDM clustering at Planck angular scales

L.A. Popa[*][†]**, C. Burigana, and N. Mandolesi**

IASF/CNR, Istituto di Astrofisica Spaziale e Fisica Cosmica, Sezione di Bologna,
Consiglio Nazionale delle Ricerche, Via Gobetti 101, Bologna I-40129, Italy
E-mail: `popa burigana mandolesi @bo.iasf.cnr.it`

ABSTRACT: We present the CMB anisotropy induced by the non-linear perturbations in the massive neutrino density associated to the non-linear gravitational clustering. We show that the non-linear time varying potential induced by the gravitational clustering process generates metric perturbations that affect the time evolution of the density fluctuations in all the components of the expanding Universe, leaving imprints on the CMB anisotropy power spectrum at subdegree angular scales. For a neutrino fraction in agreement with that indicated by the astroparticle and nuclear physics experiments and a cosmological accreting mass comparable with the mass of known clusters, we find that CMB anisotropy measurements with Planck angular resolution and sensitivity possibly combined to other precise cosmological observations will allow the detection of the dynamical, linear and non-linear effects of the neutrino gravitational clustering.

1. Introduction

The atmospheric neutrino results from the Super-Kamiokande [1] and MACRO [2] experiments indicate that neutrinos oscillate, these data being consistent with $\nu_\mu \leftrightarrow \nu_\tau$ oscillations. The small value of the difference of the squared masses ($5 \times 10^{-4}\text{eV}^2 \leq \Delta m^2 \leq 6 \times 10^{-3}\text{eV}^2$) and the strong mixing angle ($\sin^2 2\theta \geq 0.82$) suggest that these neutrinos are nearly equal in mass as predicted by many models of particle physics beyond the standard model. Also, the LSND experiment [3] support $\nu_\mu \leftrightarrow \nu_e$ oscillations ($\Delta m^2 \leq 0.2\text{eV}^2$) and other different types of solar neutrino experiments [4] suggest that ν_e could oscillate to a sterile neutrino $\nu_e \leftrightarrow \nu_s$ ($\Delta m^2 \simeq 10^{-5}\text{eV}^2$). The direct implication of neutrino oscillations is the existence of a non-zero neutrino mass in the eV range, and consequently a not negligible hot dark matter (HDM) contribution $\Omega_\nu \neq 0$ to the total energy density of the Universe.

---

[*]Speaker.
[†]Further address: Institute for Space Sciences, Bucharest-Magurele R-76900, Romania

We study the cosmic microwave background (CMB) secondary anisotropies induced by the non-linear perturbations in the massive neutrino density associated to the non-linear gravitational clustering. The extent to which the massive neutrinos can cluster gravitationally depends on their mass and the parameters of the fiducial cosmological model describing the present Universe.

The linear perturbation theory describes accurately the growth of density fluctuations from the early Universe until a redshift $z \sim 100$. The solution involves the integration of coupled and linearized Boltzmann, Einstein and fluid equations [28] that describes the time evolution of the metric perturbations in the perturbed density field and the time evolution of the density fields in the perturbed space-time for all the relevant species (e.g., photons, baryons, cold dark matter, massless and massive neutrinos). At lower redshifts the gravitational clustering becomes a non-linear process and the solution relies on numerical simulations.

Through numerical simulations, we compute the CMB anisotropy in the non-linear stages of the evolution of the Universe when clusters and superclusters of galaxies start to form producing a non-linear gravitational potential varying with time. By using a standard particle-mesh method we analyze the imprint of the dynamics of the neutrino gravitational clustering on the CMB anisotropy power spectrum in a flat ΛCHDM model with neutrino fractions $f_\nu = \Omega_\nu/(\Omega_b + \Omega_{cdm})$=0.06, 0.11, 0.16 corresponding to Ω_ν=0.022 (m_ν=0.78eV), 0.037 (m_ν=1.35 eV), 0.053 (m_ν=1.89eV), assuming three massive neutrino flavors. This model is consistent with the LSS data and the WMAP anisotropy latest measurements [5, 6] allowing in the same time a pattern of neutrino masses consistent with the results from neutrino oscillation and double beta decay experiments.

2. The neutrino gravitational infall

In the expanding Universe, neutrinos decouple from the other species when the ratio of their interaction rate to the expansion rate falls below unity. For neutrinos with masses in the eV range the decoupling temperature is $T_D \sim 1$MeV, occurring at a redsfit $z_D \sim 10^{10}$ [7]. At this time neutrinos behave like relativistic particles with a pure Fermi-Dirac phase-space distribution:

$$f_\nu(q,a) = \frac{1}{e^{E_\nu/T_\nu}+1}, \quad E_\nu = \sqrt{q^2 + a^2 m_\nu^2}, \tag{2.1}$$

where $\vec{q}$ is the neutrino comoving momentum, $\vec{q} = a\vec{p}$, $\vec{p}$ being the neutrino 3-vector momentum, E_ν is the energy of neutrino with mass m_ν and $a = 1/(1+z)$ is the cosmic scale factor evolving with the time, t (a_0=1 today).

As neutrinos are collisionless particles, they can significantly interact with photons, baryons and cold dark matter particles only via gravity. The neutrino phase space density is constrained by the Tremaine & Gunn criterion [8] that put limits on the neutrino energy density inside the gravitationally bounded objects: in the cosmological models involving a HDM component (the CHDM models) the compression fraction of neutrinos through a cluster $f(r) = \rho_\nu/\rho_{cdm}$ (where r is the cluster radius) never exceeds the background ratio Ω_ν/Ω_{cdm} [9]. Because the formation of galaxies and clusters is a dynamical time process,
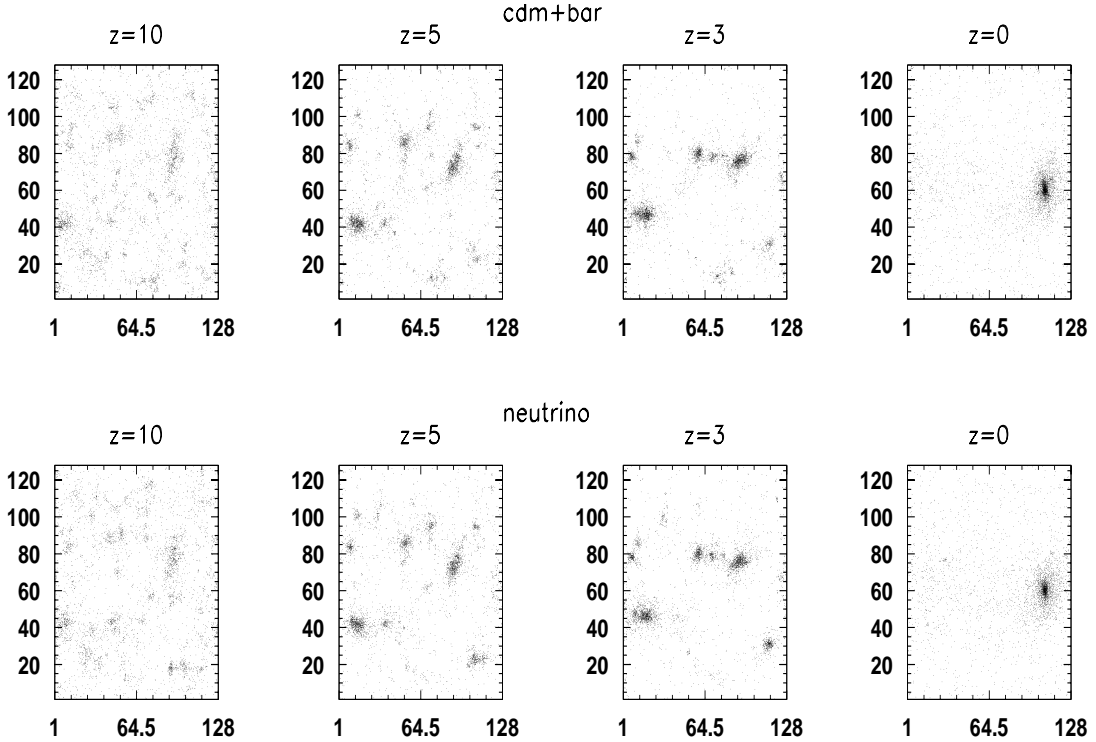
Figure 1: The evolution with the redshift of the projected mass distributions of cold dark matter plus baryons (upper row) and neutrinos (lower row) obtained from numerical simulation of 128^3 cold dark matter plus baryons (the total mass of $8 \times 10^{16} M_\odot$) and 10×128^3 neutrinos (the total mass of $4.8 \times 10^{18} M_\odot$) in a box of size 128 Mpc, for the ΛCHDM model with the neutrino fraction $f_\nu = 0.06$ ($\sum_i m_{\nu_i} \approx 0.7$ eV). [Units of axes are in Mpc].

the differences introduced in the gravitational potential due to neutrino gravitational clustering generate metric perturbations that affect the evolution of the density fluctuations of all the components of the expanding Universe. Fig. 1 presents the evolution of the projected mass distributions of cold dark matter plus baryons and neutrinos obtained from numerical simulations at few redshift values z. One can see that neutrinos are accreted by the cold dark matter and baryons, contributing in dynamic way to the gravitational clustering process.

Neutrinos cannot cluster via gravitational instability on distances below the free-streaming distance R_{fs} [10, 11, 12]. The neutrino free-streaming distance is related to the causal comoving horizon distance $\eta(a)$ through [13]:

$$R_{fs}(a) = \frac{1}{k_{fs}} = \frac{\eta(a)}{\sqrt{1 + (a/a_{nr})^2}} \, \text{Mpc}, \quad \eta(a) = \int_0^a \frac{da}{a^2 H(a)}, \qquad (2.2)$$

where a_{nr} is the value of the scale factor when massive neutrinos start to become non-relativistic ($a_{nr} = (1 + z_{nr})^{-1} \approx 3k_B T_{\nu,0}/m_\nu c^2$) and $H(a)$ is the Hubble expansion rate:

$$H^2(a) = \left(\frac{da/dt}{a} \right)^2 = \frac{8\pi G}{3} [\Omega_m/a^3 + \Omega_r/a^4 + \Omega_\Lambda + \Omega_k/a^3]. \qquad (2.3)$$
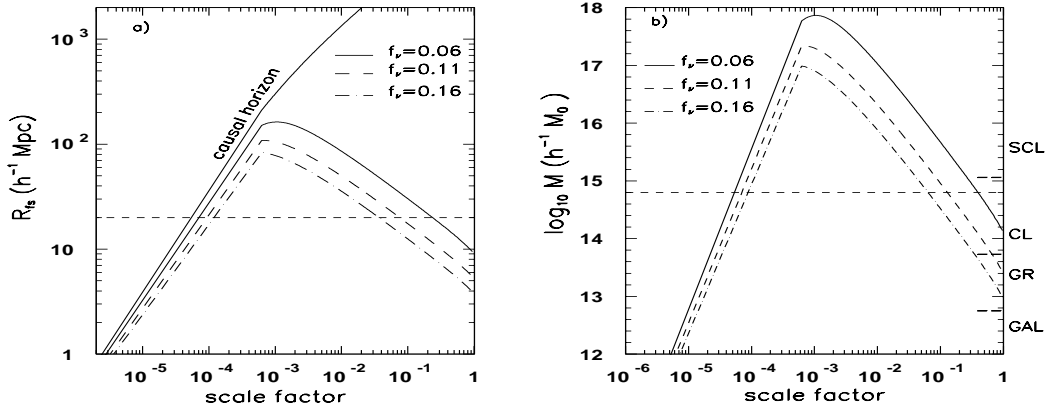
Figure 2: Panel a): dependence of the neutrino free-streaming distance R_{fs} on the scale factor. We show also a specific scale, $\lambda=20h^{-1}$Mpc, constant in comoving coordinates (horizontal dashed line) and the evolution with the scale factor of the causal horizon distance for our cosmological models. Panel b): dependence on the scale factor of the mass $M(R_{fs})$ of the perturbation at the scale R_{fs}. We show also the mass of the perturbation at the scale λ (horizontal dashed line) and indicate the typical mass ranges for galaxies (GAL), groups (GR), clusters (CL) and superclusters (SCL).

In the above equation G is the gravitational constant, $\Omega_m = \Omega_b + \Omega_{cdm} + \Omega_\nu$ is the matter energy density parameter, Ω_b, Ω_{cdm}, Ω_ν being the energy density parameters of baryons, cold dark matter and massive neutrinos, Ω_r is the radiation energy density parameter that includes the contribution from photons and relativistic neutrinos , Ω_Λ is the vacuum (or cosmological constant) energy density parameter, $\Omega_k = 1 - \Omega_m - \Omega_\Lambda$ is the energy density parameter related to the curvature of the Universe.

R_{fs} defines the minimum linear dimension that a neutrino perturbation should have in order to survive the free-streaming. In the spherical approximation, the minimum comoving mass of a perturbation that should contain clusterized neutrinos, corresponds to [14]

$$M(R_{fs}) = \frac{\pi}{6}R_{fs}^3\rho_m \approx 1.5 \times 10^{11} \, (\Omega_m h^2)(R_{fs}/\mathrm{Mpc})^3 h^{-1} M_\odot \, ,$$

where Ω_m is the matter energy density parameter.

We show in Fig. 2 the dependence of the causal horizon distance $\eta(a)$, the neutrino free-streaming distance R_{fs}, [panel a)] and of the mass $M(R_{fs})$ [panel b)] on the cosmic scale factor. The cosmological model is the ΛCHDM model with different neutrino fractions f_ν. One can see that at early times, when neutrinos are relativistic, the free-streaming distance is approximately the causal horizon distance. After neutrinos become non-relativistic ($a_{nr} \sim 10^{-4}$ for our cosmological models) the free-streaming distance decreases with time, becoming smaller than the causal horizon distance. The time behaviors of R_{fs} and $M(R_{fs})$ show that neutrino can cluster gravitationally on increasingly smaller scales at latter times. If the causal horizon $\eta(a)$ is large enough to encompass the wavelength λ, the neutrino gravitational infall perturbs the growth of the perturbations for this mode, leaving imprints in the CMB angular power spectrum. Perturbations on scales $\lambda < R_{fs}$ ($k > k_{fs}$) are damped

due to the neutrino free-streaming while the perturbations on scales $\lambda > R_{fs}$ ($k < k_{fs}$) are affected only by gravity. In the Newtonian limit, the neutrino gravitational clustering can be described as a deviation from the background by a potential Φ given by the Poisson equation:

$$\nabla^2 \Phi(\vec{r}, a) = 4\pi G a^2 \rho_m(a) \delta_m(\vec{r}, a) \,, \qquad (2.4)$$

where $\vec{r}$ is the position 3-vector, $\rho_m(a)$ is the matter density and $\delta_m(\vec{r}, a)$ is the matter density fluctuation; $\delta_m = (\rho_b \delta_b + \rho_{cdm} \delta_{cdm} + \rho_\nu \delta_\nu)/\rho_m$, where ρ_{cdm}, ρ_b, ρ_ν and δ_{cdm}, δ_b, δ_ν are the density and density fluctuations of cold dark matter particles, baryons and neutrinos.

The equations governing the motion of each particle species (cold dark matter plus baryons and neutrinos) in the expanding Universe are given by [15]:

$$\frac{d\vec{q}}{da} = -a\,H(a)\,\vec{\nabla}\Phi, \qquad \frac{d\vec{r}}{da} = \vec{q}(a^3\,H(a))^{-1}, \qquad (2.5)$$

where $\vec{q}$ is the comoving momentum and $H(a)$ is given by the equation (2.3).

The Newtonian description given by the equations (2.4) and (2.5) applies in the limit of the week gravitational field if, at each time step, the size of the non-linear structures is much smaller than the causal horizon size (the background curvature is negligible).

The cosmological models involving massive neutrinos show a characteristic scale dependence of the perturbation growth rates [16, 17, 18].

We evolve the system of baryons plus cold dark matter particles and neutrinos according to the equation (2.5) for the non-linear scales involved in the computation of the CMB anisotropy ($0.06\mathrm{Mpc}^{-1} \leq k \leq 0.52\mathrm{Mpc}^{-1}$), starting from the beginning of the non-linear regime of cold dark matter plus baryons component.

The initial positions and velocities of neutrinos and baryons plus cold dark matter particles can be generated at each spatial wave number k from the corresponding matter density fluctuations power spectra at the present time by using the Zel'dovich approximation [19]. The matter power spectra was normalized on the basis of the analysis of the local cluster X-ray temperature function [20]. We performed simulations with 128^3 cold dark matter plus baryon particles and 10×128^3 neutrinos. The neutrinos and the baryons plus cold dark matter particles was randomly placed on 128^3 grids, with comoving spacing r_0 of 0.5 h^{-1}Mpc. The high number of neutrinos and this comoving spacing ensure a precision high enough for a correct sampling of the neutrino phase space distribution [18].

According to the Zel'dovich approximation, the perturbed comoving position of each particle $\vec{r}(\vec{r}_0, a)$ and its peculiar velocity $\vec{v}(\vec{r}_0, a)$ are related to the fluctuations of the density field $\delta\rho(\vec{r}_0, a, k)$ through:

$$\vec{r}(\vec{r}_0, k, a) = \vec{r}_0 + D(k, a)\vec{d}(\vec{r}_0) \,, \quad \vec{v}(\vec{r}_0, k, a) = \dot{D}(k, a)\vec{d}(\vec{r}_0) \,, \qquad (2.6)$$
$$\vec{\nabla}\vec{d}(\vec{r}_0) = D^{-1}(k, a)\delta\rho(\vec{r}_0, k, a) \,,$$

where $\vec{r}_0$ is the coordinate corresponding to the unperturbed comoving position, $\vec{d}(\vec{r}_0)$ is the displacement field and $D(k, a)$ is the growth function of perturbations corresponding to each cosmological model.
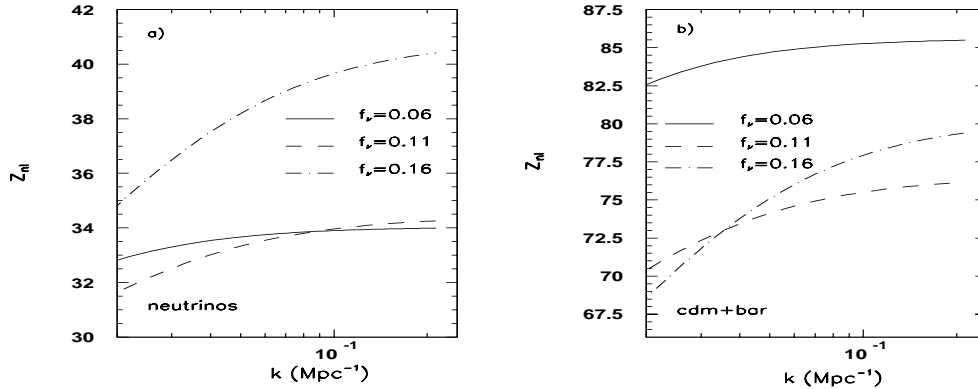
Figure 3: The scale dependence of z_{nl} on k for neutrinos (panel a) and baryons plus cold dark matter particles (panel b).

At each wave number k used in the computation of the CMB anisotropy we compute the perturbed particles comoving positions and peculiar velocities at the beginning of the non-linear regime a_{nl}, by using the set of equations (2.4)–(2.5). We assign to each particle a momentum according to the growth function, when the power of each mode is randomly selected from a Gaussian distribution with the mean accordingly to the corresponding power spectrum [21, 22, 23]. In the computation of the set of equations (2.6) we consider only the growing modes, the non-linear power spectra up to $k_{max} = 6.28$ h Mpc^{-1}, and neglect the contribution of the redshift distortions.

We show in Fig. 3 the dependence on the spatial wave number k of the redshift $z_{nl} = 1/a_{nl} - 1$ for each component. One can see from Fig. 3 that neutrinos (panel a) enter in the non-linear regime later than cold dark matter particles and baryons (panel b). Thus, the neutrino halo of the cluster starts to form after the cold dark matter plus baryon halo is advanced in the non-linear stage, causing the accretion of neutrinos from the background. At each spatial wavenumber k we evolve the particles positions and velocities according to the set of equations (2.4)–(2.5). We start this process from the scale factor a_{nl}^{cdm} at which cold dark matter particles plus baryons start to enter in the non-linear regime. At each time step, the density on the mesh is obtained from the particle positions using the Cloud-in-Cell method and equations (2.6) are solved by using 7-point discrete analog of the Laplacian operator and the FFT technique. The particle positions and velocities are then advanced in time with a time step da required by the computation of the CMB anisotropy power spectra. The system of particles was evolved until the scale factor a_{st} when it reaches its virial [24] equilibrium.

3. Imprints of neutrino gravitational clustering at PLANCK angular scales

As the anisotropy produced by the non-linear density perturbations depends on the time variations of the spatial gradients of the gravitational potential produced by different components (cold dark matter, baryons, neutrinos), we calculate the CMB anisotropy in the
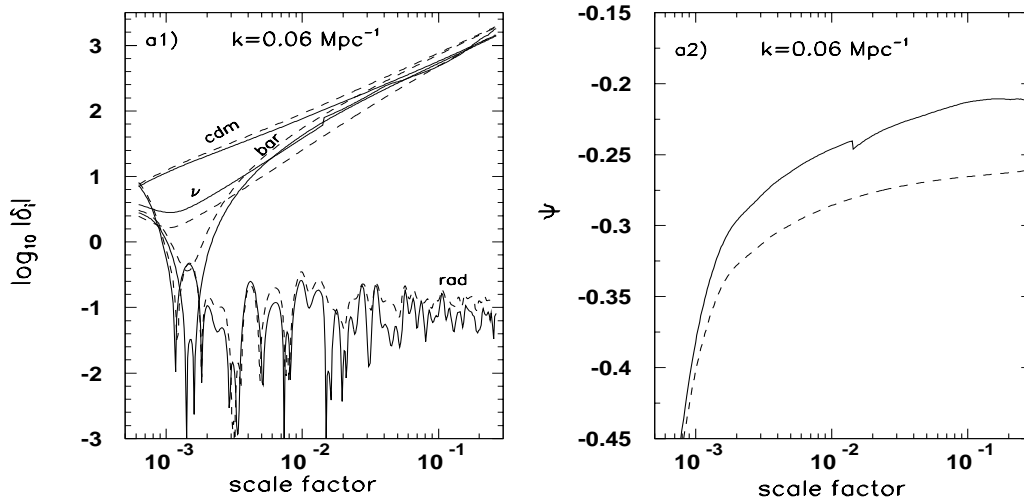
Figure 4: Panel a1): time evolution of the energy density perturbations of the different components as computed by including linear and non-linear effects of neutrino gravitational clustering (solid lines) and by neglecting the non-linear aspects of neutrino gravitational clustering (dashed lines): cold dark matter (cdm), baryons (bar), massive neutrinos (ν), and massless neutrinos plus photons (rad). Panel a2): the same as in panel a), but for the time evolution of the gravitational field [k=0.06Mpc^{-1} and $f_\nu = 0.06$].

presence of the gravitational clustering by using N-body simulation in large boxes with the side of 128 Mpc, that include all non-linear scales used in the computation of the CMB anysotropy power spectrum from $\lambda_{min} \approx 12$Mpc ($k_{max} \approx 0.52$Mpc^{-1}) to $\lambda_{max} \approx 110$ Mpc ($k_{min} \approx 0.06$Mpc^{-1}), taking into account the time evolution of all non-linear density perturbations influencing the CMB power spectrum (see also Fig. 1). One should note that λ_{max} corresponds to the comoving horizon size at the matter-radiation equality for our cosmological models ($\lambda_{eq} \approx 16\,\Omega_m^{-1}h^{-2}$Mpc). The non-linear structures are assumed to be formed by two components: cold dark matter plus baryons and neutrinos in the form of three massive neutrino flavors, both components evolving in the gravitational field created by themself. For the purpose of this work we neglect the hydrodinamical effects [25]. The neutrino gravitational clustering can affect both the homogeneous and the inhomogeneous components of the gravitational field. The changes in the homogeneous component of the gravitational field are determined by the changes of the energy density of neutrinos and cold dark matter particles plus baryons. They affect the Hubble expansion rate, the sound horizon distance and the neutrino free-streaming distance. The changes in the inhomogeneous component of the gravitational field are determined by the changes in the energy density for all matter components and the changes in the neutrino phase space distribution function. They affect the growth of the energy density perturbations of cold dark matter, baryons, photons, massive and massless neutrinos. Panel a1) of Fig. 4 presents the evolution with the scale factor of the energy density perturbations of different components in the non-linear regime, for the mode $k = 0.06$ Mpc^{-1} (solid lines). For comparison, we plot also (dashed lines) the energy density perturbations of the different components obtained
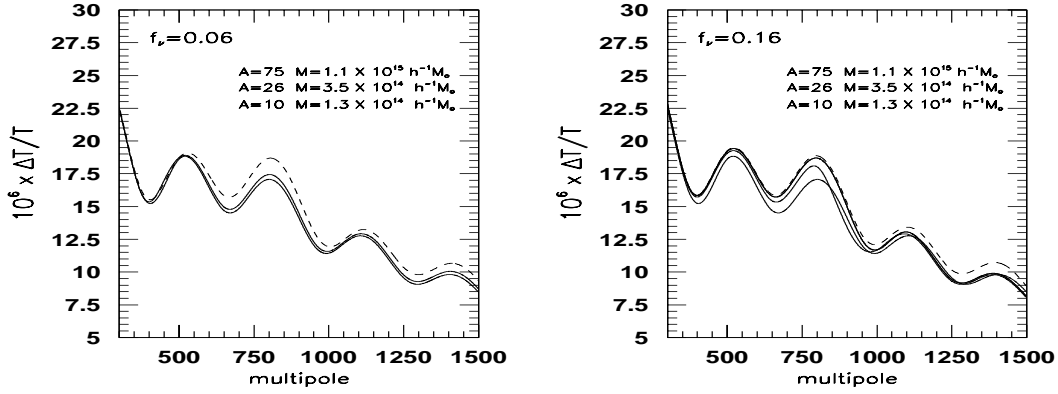
Figure 5: The imprint of the neutrino linear and non-linear gravitational clustering on the CMB anisotropy power spectrum expressed in terms of $\Delta T/T$ obtained for the filtering perturbation with the mass M. We report in the panels the richness of these perturbations from the bottom to the top according to the increasing of the power at multipoles about $\ell \sim 750$. In each panel, the dashed line corresponds to the fiducial ΛCHDM cosmological model, without including the non-linear effects of neutrino gravitational clustering.

for the same mode k by neglecting non-linear aspects of neutrino gravitational clustering (linear regime). Panel a2) of Fig. 4 presents the evolution with the scale factor of the scalar potential Ψ of the conformal Newtonian gauge line element, that plays the role of the gravitational potential in the Newtonian limit [26, 27], by including (solid line) or not (dashed line) the non-linear effects of neutrino gravitational clustering (for the transformation relation between the scalar potentials of the synchronous gauge and conformal Newtonian gauge see equation (18) from [28]). As we have shown before, the difference in the evolution of a perturbation mode k depends on how this mode relates to the neutrino free-streaming wave number k_{fs}. Considering that our simulation at each time step is a sample of the evolution of the matter in the non-linear regime, we study the imprint of the gravitational clustering on the CMB anisotropy power spectrum by smoothing the density field obtained from simulation at each time step with a filter with the scale R_{fs} corresponding to the cluster mass value $M(R_{fs})$. For each non-linear mode k only the perturbations with the mass $M \leq M(R_{fs})$ are taken into account for the computation of the CMB anisotropy power spectrum. Fig. 5 presents some of our computed CMB anisotropy power spectra obtained when different filtering mass values $M(R_{fs})$ are considered. It is usual to use the Coma cluster as the mass normalization point ($M_{\text{Coma}} = 1.45 \times 10^{15} \text{h}^{-1} M_{\odot}$); for the Coma cluster we assume a richness $\mathcal{A}_{\text{Coma}}=106$. According to [29], the relation between the mass of the perturbation and the richness $\mathcal{A}$ of the corresponding cluster can be written in the form

$$M = M_{\text{Coma}} \frac{\mathcal{A}}{\mathcal{A}_{\text{Coma}}} = 1.45 \times 10^{15} \left(\frac{\mathcal{A}}{106} \right) h^{-1} M_{\odot} \,.$$

By comparing the angular power spectra obtained including or not the non-linear effects of neutrino gravitational clustering, we find a decrease of the CMB angular power spectrum induced by the neutrino non-linear gravitational clustering of $\Delta T/T \approx 10^{-6}$ for angular resolutions between ~ 4 and 20 arcminutes, depending on the cluster mass and neutrino

fraction f_ν.

Clearly, new high sensitivity and resolution anisotropy experiments will have the capability to detect the neutrino gravitational clustering effect. In particular, the instruments on-board the ESA PLANCK satellite [1] will measure the CMB angular power spectrum with very high sensitivity up to multipoles $\ell \sim 1000 - 2000$ with a stringent control of the systematic effects. Fig. 6 compares PLANCK and WMAP [2] performances. The CMB angular power spectrum is reported without beam smoothing and by taking into account the beam window functions of several PLANCK frequency channels and of the highest WMAP frequency channel (which is very close to that of the LFI 70 GHz channel). The corresponding angular power spectra of the residual nominal white noise (i.e. after the subtraction of the expection of its angular power spectrum) are also displayed. Of course, binning the power spectrum on a suitable range of multipoles, as usual at high ℓ, will allow to recover the CMB power spectrum also at multipoles higher that those corresponding to the crossings between the noise and CMB power spectra reported in the figure [3].

The characteristic angular scale left by the the neutrino gravitational clustering on the CMB anisotropy power spectrum is given by

$$\theta = \frac{R_{fs}}{\eta_0 - \eta(a)}\,,$$

where R_{fs} is the scale of the filtering perturbation with the mass $M(R_{fs})$, $\eta(a)$ is the particle horizon distance at the time at which the non-linear perturbation mode k cross the horizon and η_0 is the particle horizon at the present time. Fig. 7 (left panel) presents the evolution of the characteristic scale θ and of the corresponding multipole order of the CMB anisotropy power spectrum with the mass $M(R_{fs})$.

Fig. 7 (right panel) presents few confidence regions of the $f_\nu - M$ parameter space that can be potentially detected by the PLANCK surveyor by using the CMB anisotropy measurements in the presence of the gravitational clustering, under the hypothesis that the other cosmological parameter can be measured with other observations (grey regions) and by using the PLANCK data to jointly determine f_ν, M and the other cosmological parameters (solid lines). We consider for this computation only the PLANCK "cosmological" channel between 70 and 217 GHz, a sky coverage $f_{sky} = 0.8$ and neglect for simplicity the foreground contamination [18]. By assuming known the other main cosmological parameters, we obtain a neutrino fraction $f_\nu \approx 0.011 \pm 0.007$ for an accreting mass $M \approx (8.2 \pm 3.1) \times 10^{14} h^{-1} M_\odot$ (errors at 68% confidence level). By assuming known the other main cosmological parameters, we obtain a neutrino fraction $f_\nu \approx 0.011 \pm 0.007$ for an accreting mass $M \approx (8.2 \pm 3.1) \times 10^{14} h^{-1} M_\odot$ (errors at 68% confidence level). PLANCK surveyor will have in principle the capability to measure the non-linear imprints of the neutrino gravitational clustering on the CMB anisotropy power spectrum for a neutrino mass range in agreement with that indicated by the astroparticle and nuclear physics

---

[1] http://astro.estec.esa.nl/Planck

[2] http://lambda.gsfc.nasa.gov

[3] At ℓ higher than $\simeq 1500 - 2000$ the confusion noise from extragalactic source fluctuations dominates over the instrumental noise, while Galactic foregrounds are relevant at multipoles less than few hundreds.
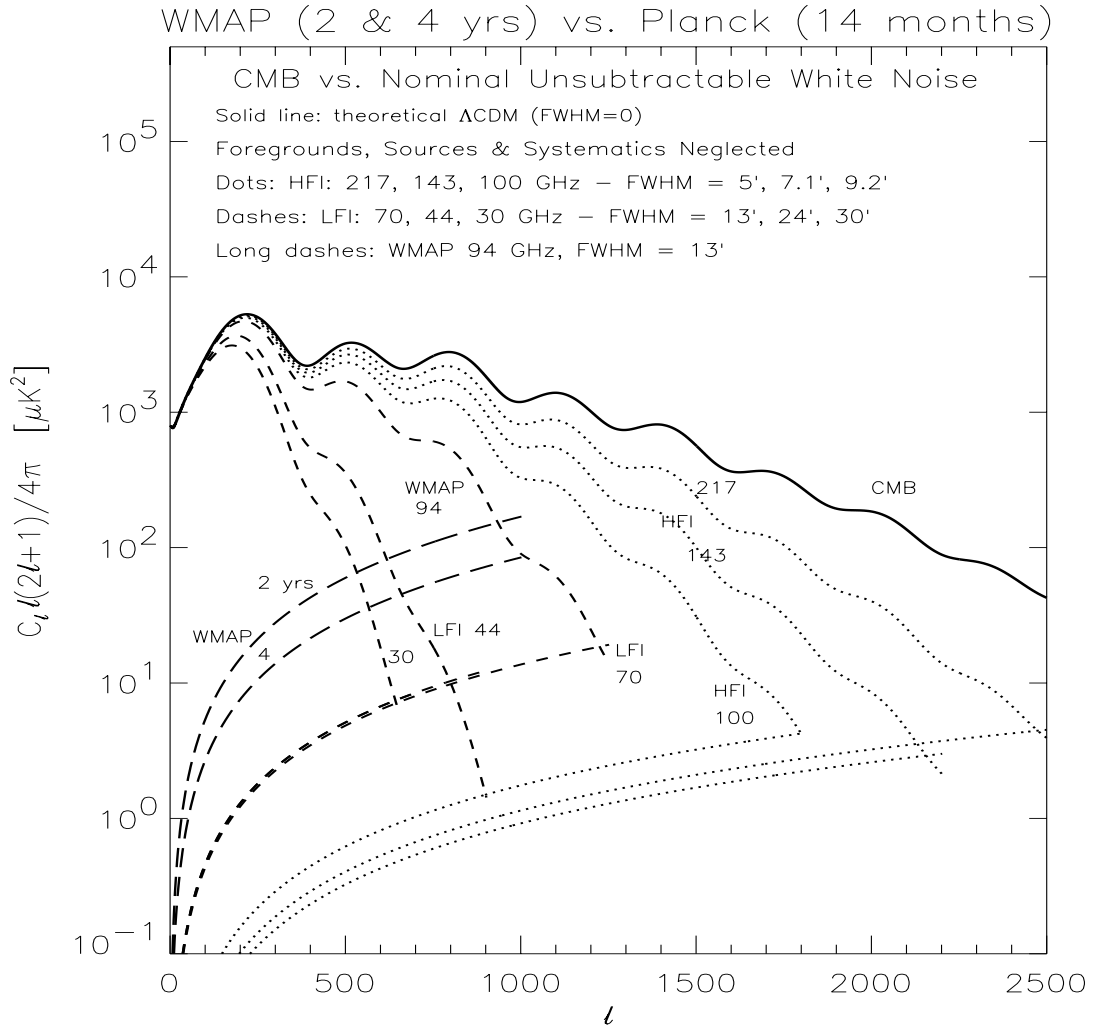
Figure 6: Comparison between PLANCK and WMAP resolution and sensitivity. For each considered frequency channel, the crossing between the CMB convolved angular power spectrum and the unsubtractable instrumental white noise angular power spectrum indicates the multipole value where the signal to noise ratio (ℓ by ℓ) is close to unity.

experiments and a cosmological accreting mass comparable with the mass of the known clusters. Of course, even with the high sensitivity and resolution of PLANCK it is hard to firmly constrain f_ν and M by jointly recovering the other cosmological parameters, a goal that can be achieved in combination with other precise cosmological information, such as galaxy large scale structure surveys, measures of element abundances from big-bang nucleosynthesis and Type 1a supernovae observations.

4. Conclusions

We study the CMB anisotropy induced by the non-linear perturbations in the massive neutrino density associated to the non-linear gravitational clustering. Through numerical
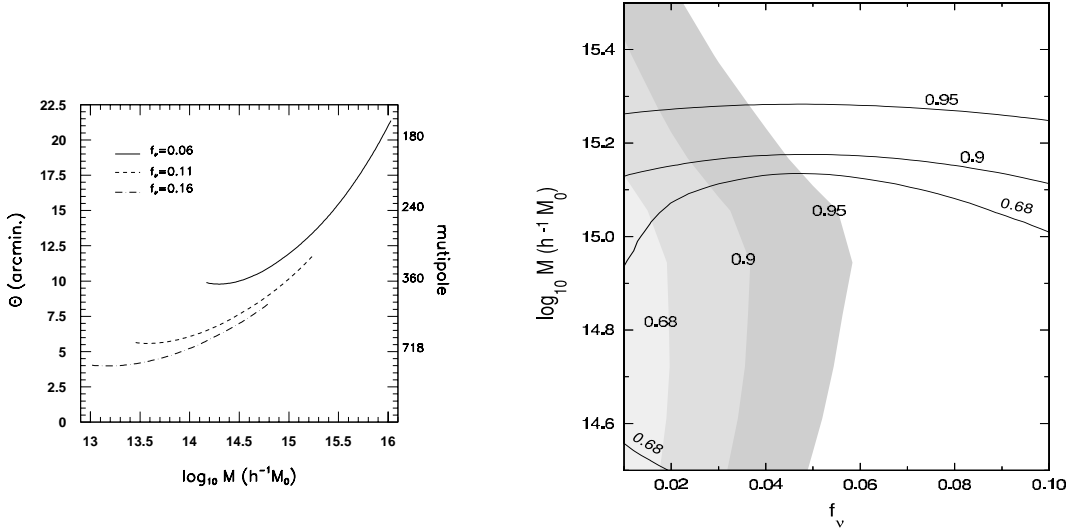
Figure 7: Left panel: evolution of the characteristic angular scale θ of the neutrino gravitational clustering with $M(R_{fs})$ for different neutrino fractions. We report also the corresponding multipole orders $l \sim \theta^{-1}$ of the CMB anisotropy power spectrum. Right panel: confidence regions of the $f_\nu - M$ parameter space as potentially detectable by PLANCK by using the CMB anisotropy measurements in the presence of the gravitational clustering assuming known the other main cosmological parameters (grey regions) or by jointly recover f_ν, M and the other main cosmological parameters (solid lines).

simulations, we compute the CMB anisotropy angular power spectrum in the non-linear stages of the evolution of the Universe when clusters and superclusters start to form, producing a non-linear time varying gravitational potential.

We found that the non-linear time varying potential induced by the gravitational clustering process generates metric perturbations that affect the time evolution of the density fluctuations in all the components of the expanding Universe, leaving imprints on the CMB anisotropy power spectrum at subdegree angular scales. The magnitude of the induced anisotropy and the characteristic angular scale depends on how each non-linear mode k of the perturbations relates to the neutrino free-streaming wavenumber k_{fs} at each evolution time step. By smoothing the density field obtained from simulations with a filter with the scale corresponding to the cluster scale, we find an imprint on the CMB anisotropy power spectrum of amplitude $\Delta T/T \approx 10^{-6}$ for angular resolutions between ~ 4 and 20 arcminutes, depending on the cluster mass and neutrino fraction f_ν.

This result suggests that the CMB anisotropy experiments with such levels of sensitivities and angular resolutions should detect the dynamical effect of the non-linear gravitational clustering. For a neutrino fraction in agreement with that indicated by the astroparticle and nuclear physics experiments and a cosmological accreting mass comparable with the mass of known the clusters, we find that CMB anisotropy measurements with PLANCK angular resolution and sensitivity in combination with other precise cosmological observations will allow the detection of the dynamical, linear and non-linear, effects of the neutrino gravitational clustering.

Acknowledgments

References

[1] Y. Fukuda, et al. (Super-Kamiokande Coll.), 1998, Phys. Rev. Lett., 81, 1562

[2] M. Ambrosio, et al. (MACRO Coll.), 1998, Phys. Lett. B, 478, 5

[3] C. Athanassopoulos, et al., 1998, Phys. Rev. Lett., 81, 1744

[4] J.N. Bahcall, P.I. Krastev, A.Yu. Smirnov, 1998, Phys. Rev. D, 58, 096016.

[5] D.N. Spergel, et al., 2003, ApJS, 148,175

[6] L. Verde, et al., 2003, ApJS, 148, 195

[7] K. Freese, E.W. Kolb, M. Turner, 1983, Phys. Rev. D, 27, 1689

[8] S. Tremaine & J.E. Gunn, 1979, Phys. Rev. Lett., 42, 407

[9] L.A. Kofman & A.A. Starobinskii, 1985, Sov. Astron. Lett., 434, L1

[10] J.R. Bond, G. Efstathiou, J. Silk, 1980, Phys. Rev. Lett., 45, 1980

[11] J.R. Bond & A.S. Szalay, 1983, ApJ, 274, 443

[12] C.P. Ma, 2000, in Neutrinos in Physics and Astrophysics: From 10^{-33} to 10^{28} cm, ed. Paul Langacker (Singapore: World Scientific), 504

[13] S. Dodelson, E. Gates, A. Stebbins, 1996, ApJ, 467, 10

[14] W.E. Kolb & M. Turner, 1990, in The Early Universe (Addison-Wesley Publishing)

[15] J. Gleb & E. Bertshinger, 1994, ApJ, 436, 467

[16] C.P. Ma, ApJ, 1996, 471, 13

[17] W. Hu & D.J. Eisenstein, 1998, ApJ, 498, 497

[18] L.A. Popa, C. Burigana, N. Mandolesi, 2001, ApJ, 558, 10

[19] Ya.B. Zel'dovich, 1970, A&A, 5, 84

[20] V.R. Eke, S. Cole, C.S. Frenk, 1996, MNRAS, 282, 263

[21] Y. Hoffman & R. Ribak, 1991, ApJL, 380, 5

[22] G. Ganon & Y. Hoffman, 1993, ApJL, 415, 5

[23] E. Bertschinger, 1995, http : //arcturus.mit.edu/cosmics

[24] A.J. Peacock, 2000, in Cosmological Physics (Cambridge: University Press)

[25] V. Quilis, J.M Ibanez, D. Saez, 1995, MNRAS, 277, 445

[26] J.M. Bardeen, 1980, Phys. Rev. D, 22, 1882

[27] H. Kodama & M. Sasaki, 1984, Prog. Theor. Phys. Suppl., 78, 1

[28] C.P. Ma & E. Bertschinger, 1995, ApJ, 455, 7

[29] A. Kashlinsky, 1998, ApJ, 492, 1